



New Method of Materials Flow Calculation for Double-String SLCI Type Cement Plant (Part 2: Suspension Preheater and Calciners)

Prihadi Setyo Darmanto^{1,*}, Izzan Hakim Muzakki¹, I Made Astina¹, Firman Bagja Juangsa¹, Alfi Amalia² & Arief Syahlan²

¹Faculty of Mechanical and Aerospace Engineering, Institut Teknologi Bandung, Jalan Ganesa 10, Bandung 40132, Indonesia

²Indonesia Cement and Concrete Institute, Jalan Ciangsana Raya, Bogor, Indonesia

*E-mail: prihadisetyo@gmail.com

Highlights:

- A new approach for calculating detailed materials and heat flows in a double-string type cement plant with separate and in-line calciners (SLC-I) is presented in two parts (Part 1 and Part 2).
- The least squares method was used for solving the obtained overdetermined system equations, based on the measurement of kiln feed and gas temperatures.
- With this method the detailed materials and heat flows as well as the separating efficiency of each cyclone, which cannot be measured directly in the plant during operation, can be approached with an error of heat balance smaller than 1%.
- The obtained results can be used for operational control needs, designing and analyzing new equipment, numerical study of the suspension preheater, and even modification of existing equipment.
- The second part of the study focused on the detailed heat and materials flows in each cyclone of the suspension pre-heater and the calciners, including their impact on operational practice.

Abstract. In many industries, energy auditing is important as the basis for controlling processes and designing additional equipment or modifying an existing plant. However, it requires detailed data of the materials flow, which often cannot be determined easily by direct measurement due to high-temperature limitations. This paper presents the second part of an integrated study to perform energy auditing in a separate line and in-line calciners (SLC-I) type cement plant. The second part of this study, as presented in this paper, focused on the materials flow calculation for eight separate cyclones and two calciners. The least square method was employed for solving the obtained overdetermined system equations. Using the operation data from Part 1 of the study, calculation of the detailed materials flow in each cyclone was executed. The results showed that the separation efficiency of cyclones 1A, 2A, 3A, 4A and 1B, 2B, 3B, 4B was 93.86%, 89.80%, 84.41%, 81.98% and 93.96%, 88.70%, 88.53%, 80.72% respectively and the estimated calcination percentage of kiln feed coming out of the ILC and the SLC was 85.3% and 56.3%, respectively. These values are impossible to be measured directly in the cyclones and calciners during plant operation.

Keywords: *cyclone; least square; overdetermined system; separation efficiency; suspension preheater.*

1 Introduction

As mentioned in the first part of this research, a modern cement plant consists of a suspension preheater (SP), calciners, a kiln, and a clinker cooler. The production of cement is energy-intensive. In order to improve the energy consumption, it is essential to conduct a precise heat consumption analysis of the plant to optimize heat conservation and efficiency, as mentioned by Rivendra, *et al.* [1] and Anantharaman [2]. Therefore, energy auditing of cement plants is conducted to identify opportunities to reduce heat consumption, improve productivity and environmental protection, and plan the necessary conservation efforts, as proposed by Avami and Sattari [3] and Parinya and Unchalee [4]. Some efforts for waste materials utilization have been reported by Nørskov, *et al.* [5], Mikulčić, *et al.* [6], and Chao, *et al.* [7]. The utilization of alternative materials as clinker substitute and to reduce the production cost was observed intensively by Kourounis [8], Varma and Gadling [9], Ghassan, *et al.* [10], and Allahverdi and Salem [11]. A number of works on heat waste conservation for producing electric power have been conducted by Ayu, *et al.* [12], Hendi and Sigit [13], and Kawasaki Plant System Ltd. [14]. The application of the Kalina cycle for obtaining the most efficient power plant was shown by Ali and Mohammad [15]. Integration of a cement plant with other plants to produce other products and electricity is discussed in Firman and Muhammad [16] and Firman, *et al.* [17]. Heat efficiency improvements were made by modifying processes and equipment. Top cyclone preheater modification has been conducted to increase its separation efficiency and clinker to kiln-feed ratio as well as to reduce return dust, which can contaminate the fine coal in coal mills, as reported by Paa and Darmanto [18] and Darmanto, *et al.* [19].

Mikulčić, *et al.* [20] and Amila, *et al.* [21] have reported results from modeling the calcination process in the calciner and modification of the calcination process using co-fuel combustion. Reports concerning equipment modification to increase process efficiency have been published, such as modification of the tertiary duct, and modernization of the kiln using a pyroclone calciner has been reported by Grzegorz, *et al.* [22] and Claus [23]. The development of the design concept as well as the evolution of the main burner has been proposed by Xavier D'Hubert [24]. To minimize cost and avoid production stops, these studies used computational fluid dynamics (CFD) to understand the mechanism of any equipment modification. CFD simulations have been reported by Niki and Akshey [25] and Hrvoje, *et al.* [26].

Almost all of the research mentioned above required precise and accurate data such as the mass flowrate of gas and solid material entering into the equipment, but the source of these data is rarely mentioned. Obtaining precise input data from currently active cement manufacturing plants remains a prevalent issue. It is

hampered by the limitations of measurement instruments and methods in very high-temperature conditions, which can sometimes not be used while the plant is running.

Input data for setting up a simulation can be obtained from possible direct measurement in a cement plant. These data consist of operational parameters such as feed rate, clinker production, fuel mass rate, air consumption rate for transporting fuel, clinker cooling air rate, and equipment surface temperature. Meanwhile, the materials and gas flows between two interconnected devices cannot be measured directly when the plant is in operation. For example, between the cyclones of the suspension preheater (SP), between the cyclones and the calciner, and between the kiln and the clinker cooler. Materials flow data such as the input and output materials flow rates in each cyclone stage and in the calciners are necessary for developing new designs, process simulation, and modification of cyclones and calciners.

The difficulties in making direct measurements in cement manufacturing equipment are related to technical limitations such as high temperature, dust in the environment, and others, as mentioned in the report of Edoardo, *et al.* [27]. Furthermore, the separation efficiency of each cyclone is closely related to the rate of materials and heat flows in the whole SP and the calciners. Due to the difficulty of direct measurement, normally, the design values are used in studies. However, the design values certainly do not match the conditions during practical equipment operation when the factory is running. Thus, parametrization based on real operating condition values is necessary to obtain a realistic approach for preheater system design modification.

The literature survey conducted in this study indicated that studies on the direct measurement of materials flow of the cyclone separator in a cement preheater are limited in number and scope. Thus, the main objective of the second part of this research was to develop a new method for calculating the detailed materials (gas and solid) flows in each cyclone and in the calciner in a separated line with in-line calciners (SLC-I) preheater system, without performing direct mass flow rate measurements on the related equipment. In order to simplify the modeling and calculation results, the conservation equations of the cyclone preheater were formed as a matrix and solved using the least-square method. Through this proposed method, the materials flow value as well as the separation efficiency value for the cyclones can be calculated with heat balance error smaller than 1%. Through this study, as the novelty of this research, we also expect to provide more accurately data required for designing new equipment, modification of equipment, process simulation, plant operation control, and detailed heat auditing.

2 Methods

2.1 Suspension Preheater and Calciners

The configuration of cement plants varies depending on the plant design, especially related to the suspension preheater and the calciner. According to the classification proposed by Schmidt [28], the configuration of the studied dry process cement plant is limited to the separate line calciner with in-line calciner (SLC-I) type shown in Figure 1.

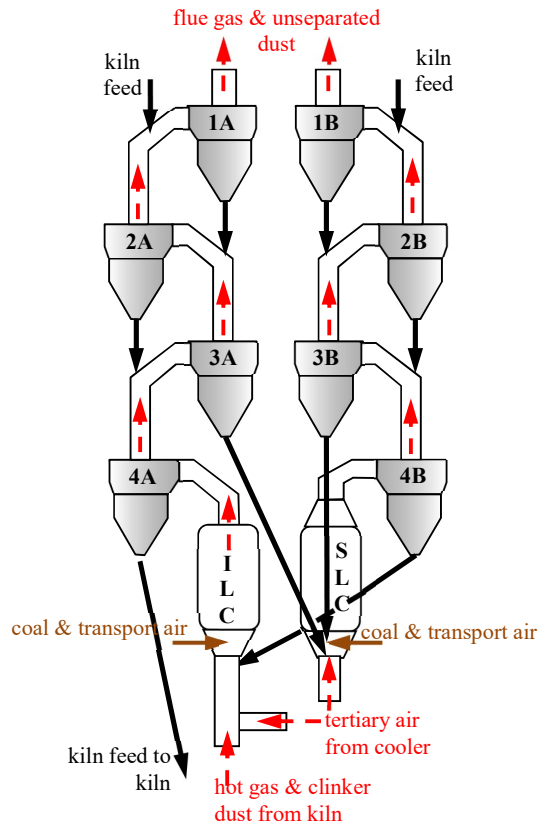


Figure 1 Schematic diagram of configuration of SLC-I preheater and calciners.

The preheater consists of two strings. Each string has four cyclone separators installed in series and one calciner unit. The string connected to the kiln is called the kiln string or A-string, while the calciner is called an in-line calciner (ILC). The string separated from the kiln is called the B-string and the calciner is called

a separated line calciner (SLC). In Figure 1 it can be seen that the kiln feed is inserted into the SP through the riser duct of the top cyclone of each string. The material coming out of cyclones 3A and 3B are first flowed towards the SLC and then separated by cyclone 4B before entering into the ILC. From the ILC, the kiln feed is separated by cyclone 4A and goes on to the kiln for further processing to become clinker.

2.2 Conservation Equations for the Suspension Preheater

The flow of solid materials and gas through the SP and calciners is presented in Figure 1 and its related mass conservation equation can be written as follows:

$$\begin{aligned}
 & m_{kf-A} + m_{kf-B} + m_{hg-k-ILC} + m_{clid-k-ILC} + m_{comb-air-ILC} \\
 & \quad + m_{comb-air-SLC} + m_{clid-c-ILC} + m_{clid-c-SLC} \\
 & \quad + m_{coal-ILC} + m_{coal-SLC} + m_{tr-air-ILC} + m_{tr-air-SLC} = \\
 & m_{sep-kf-4A} + m_{H_2O-kf-1A} + m_{H_2O-kf-1B} + m_{unsep-kf-1A} + \\
 & m_{unsep-kf-1B} + m_{hg-A} + m_{hg-B} + m_{gas-kf-A} + m_{gas-kf-B}
 \end{aligned} \tag{1}$$

The flow of mass entering the SP and the calciners consists of:

1. Mass flow rate of kiln feed through strings A and B, m_{kf-A} and m_{kf-B}
2. Mass flow rate of hot gas from kiln to in-line calciner (ILC), $m_{hg-k-ILC}$
3. Mass flow rate of clinker dust from kiln back to SP through ILC, $m_{clid-k-ILC}$
4. Mass of combustion air from the cooler to ILC, $m_{comb-air-ILC}$
5. Mass of combustion air from cooler to SLC, $m_{comb-air-SLC}$
6. Mass of clinker dust from cooler to ILC, $m_{clid-c-ILC}$
7. Mass of clinker dust from cooler to SLC, $m_{clid-c-SLC}$
8. Mass of fine coal to ILC, $m_{coal-ILC}$
9. Mass of fine coal to SLC, $m_{coal-SLC}$
10. Mass of transporting air of the fine coal to ILC, $m_{tr-air-ILC}$
11. Mass of transporting air of the fine coal to SLC, $m_{tr-air-SLC}$
12. Mass of transporting air of the fine coal to SLC, $m_{tr-air-ILC}$

The materials flow exiting from the SP and the calciners consists of:

1. Mass flow rate of separated kiln feed from cyclone 4A, $m_{sep-kf-4A}$.
2. Mass flow rate of evaporating water content in kiln feed (vapor) through strings A and B, $m_{H_2O-kf-1A}$ and $m_{H_2O-kf-1B}$.
3. Mass flow rate of unseparated kiln feed from top cyclone of strings A and B, $m_{unsep-kf-1A}$ and $m_{unsep-kf-1B}$.
4. Mass of hot gas through top cyclone of strings A and B, m_{hg-A} and m_{hg-B} .
5. Mass of gas obtained from kiln feed calcination process through top cyclone of strings A and B, $m_{gas-kf-A}$ and $m_{gas-kf-B}$.

It should be noted that the values of $m_{sep-kf-AA}$ and $m_{clid-k-ILC}$ are known by solving the kiln mass conservation equation. The flow of heat equation in the SP and the calciners can be presented as follows:

$$\begin{aligned}
 & En_{kf-A} + En_{kf-B} + En_{hg-k-ILC} + En_{clid-k-ILC} + En_{coal-ILC} + \\
 & En_{comb-air-ILC} + En_{clid-c-ILC} + En_{tr-air-ILC} + En_{coal-comb-SLC} + \\
 & En_{comb-air-SLC} + En_{clid-c-SLC} + En_{coal-SLC} + En_{tr-air-SLC} = \\
 & En_{kf-4A-k} + En_{vapor-kf-A} + En_{vapor-kf-B} + En_{evap-kf-A} + \quad (2) \\
 & En_{evap-kf-B} + En_{unsep-kf-A} + En_{unsep-kf-B} + En_{gas-kf-A} + \\
 & + En_{gas-kf-B} + En_{evap-H_2O-coal-A} + En_{evap-H_2O-coal-B} \\
 & + En_{hg-A} + En_{hg-B} + En_{calc-SPC} + Q_{loss-SP}
 \end{aligned}$$

The heat flow into the SP consists of:

1. Heat of kiln feed entering to SP, $En_{kf} = En_{kf-A} + En_{kf-B}$, Eq. (12) in Part 1.
2. Heat of hot gas from kiln, $En_{hg-k-ILC}$, which can be calculated using Eq. (A12) in Part 1, Appendix 1.
3. Heat of return clinker dust from kiln, $En_{clid-k-ILC}$, represented by Eq. (A19) in Part 1, Appendix 1.
4. Heat of combustion air from cooler to ILC, $En_{comb-air-ILC}$, as mentioned in Eq. (A6) in Part 1, Appendix 1.
5. Heat of return clinker dust from cooler back to ILC, $En_{clid-c-ILC}$, represented by Eq. (A9) of Part 1, Appendix 1.
6. Heat of coal transporting air for ILC, as mentioned in Eq. (3):

$$En_{tr-air-ILC} = m_{tr-air-ILC} * h_{air}(T_{air}) \quad (3)$$

7. Heat of fine coal combustion result in ILC, $En_{coal-comb-ILC}$, which can be evaluated using Eq. (4):

$$En_{coal-comb-ILC} = m_{coal-ILC} * NHV_{coal} \quad (4)$$

8. Heat of combustion air from cooler to SLC, $En_{comb-air-SLC}$, as mentioned in Eq. (A8) in Part 1, Appendix 1.
9. Heat of return clinker dust from cooler back to SLC, $En_{clid-c-SLC}$, represented by Eq. (A10) in Part 1, Appendix 1.
10. Heat of coal transporting air for SLC as mentioned in Eq. (5):

$$En_{tr-air-SLC} = m_{tr-air-SLC} * h_{air}(T_{air}) \quad (5)$$

11. Heat of the fine coal combustion result in ILC, $En_{coal-comb-ILC}$, which can be evaluated using Eq. (6):

$$En_{coal-comb-SLC} = m_{coal-SLC} * NHV_{coal} \quad (6)$$

The heat flows from the SP and the calciners consist of:

1. Heat flow of unseparated kiln feed by lowest cyclone of string A, Eq. (A14) in Part 1, Appendix 1.
2. Heat of evaporated water content in kiln feed as written in Eq. (18a) and Eq. (18b) in Part 1.
3. Heat flow of evaporating process of kiln feed water content as formulated by Eq. (7):

$$En_{evap-kf} = En_{evap-kf-A} + En_{evap-kf-B} = m_{H_2O-k} * h_{fg} \quad (7)$$

where m_{H_2O-kf} mentioned in Eq. (7) is the mass of evaporated water content in the kiln feed and h_{fg} is the enthalpy of the water evaporation process.

4. Heat flow of unseparated kiln feed through the top cyclones of strings A and B, as mentioned in Eq. (19 a) and Eq. (19b) in Part 1.
5. Heat of gas of kiln feed calcination and burning processes through the top cyclones of strings A and B dominated by CO₂. Its value is approximated by Eq. (20) in Part 1.
6. Evaporation heat of water content in fine coal exiting from the top cyclones, expressed in Eq. (8):

$$En_{evap\ 2O-coal-A} + En_{evap\ 2O-coal-B} = (m_{H_2O-coal-ILC} + m_{H_2O-coal-SLC}) * h_{fg} \quad (8)$$

where $m_{H_2O-coal-IL} = H_2O_{coal} * m_{coal-ILC}$ and $m_{H_2O-coal-SL} = H_2O_{coal} * m_{coal-SLC}$ are water content of fine coal supplied to ILC and SLC, where H_2O_{coal} is the percentage by mass of water in the fine coal used as fuel for the clinker plant.

7. Heat flow of coal combustion process gas exiting from the top cyclones $En_{hg-A} + En_{hg-B}$, as formulated in Part 1 by Eq. (17).
8. Heat of calcination process in SP and calciners, $En_{calc-SPC}$, as presented in Eq. (9):

$$\begin{aligned} En_{calc-SPC} &= En_{calc-3A} + En_{calc-3B} + En_{calc-4A} + En_{calc-4B} \\ &\quad + En_{calc-ILC} + En_{calc-SLC} \\ &= (\%Calc_{3A} + \%Calc_{3B} + \%Calc_{4A} + \%Calc_{4B} \\ &\quad + \%Calc_{ILC} + \%Calc_{SLC}) * En_{calc} \end{aligned} \quad (9)$$

where $En_{calc-3A}$, $En_{calc-3B}$, $En_{calc-4A}$, $En_{calc-4B}$, $En_{calc-ILC}$, and $En_{calc-SLC}$ are the heat of the calcination process in cyclones 3A, 3B, 4A, 4B, ILC and SLC while $\%Calc_{3A}$, $\%Calc_{3B}$, $\%Calc_{4A}$, $\%Calc_{4B}$, $\%Calc_{ILC}$ and $\%Calc_{SLC}$ are the respective related percentages of the kiln feed calcination degree.

9. Heat loss by radiation and convection Q_{loss_SP} through SP and calciner surface area (A_{SP}), which can be approached by Eq. (24) in Part 1 by substituting A_{tot} with A_{SP} .

Calculating the mass and heat flows in each cyclone separator and in the calciners is very useful for plant operation monitoring and parametric design as well as

equipment modification. Their formulations are derived one by one in Appendix 1.

2.3 Calculation Methodology

To solve the materials flow rate in each main equipment in more detail (e.g. the detailed materials flow rate in each cyclone of the SP and the calciners) Eqs. (A1) to (A20) in Appendix 1 should be used. Unfortunately, although the formulation of the mass and heat conservation for each cyclone and calciner has been derived (Appendix 1), the values of materials and heat flow in cyclones 2A, 2B, 3A, 3B, 4A, 4B and the calciners cannot be calculated sequentially. This is due to the unknown variables of the kiln feed mass separated by cyclones 2A, 2B, 3A, 3B, and 4B exiting from ILC and SLC, and the unseparated kiln feed from cyclones 3A, 3B, 4A and 4B. These eleven unknown parameters are interdependent and need to be solved simultaneously. In order to evaluate all eleven parameters simultaneously, the equations of mass and heat balance of cyclones 2, 3, 4 of strings A and B and the calciners (ILC and SLC) are used, written in matrix form as follows:

$$[A] \times [X] = [B] \quad (10)$$

The elements of matrices $[A]$, $[X]$, and $[B]$ are presented in Appendix 2. Matrix $[A]$ 16 x 11 is a constant as a multiplier of unknown variables, while matrix $[B]$ 11 x 1 is a constant resulting from the known constant value of Eq. (10). Matrix $[X]$ 1 x 11 is the variable that should be solved. Eq. (10) is a representation of 16 linear equations with eleven of unknown variables. Furthermore, because the rank of $[A]$ is smaller than the rank of the conjunction of $[A]$ and $[B]$, according to Anton and Rorres [28], this system of equations is called an overdetermined equation system. Overdetermined equation systems usually have inconsistent variables, but the solution can still be approached using the least square method to find the value to fulfill the equation of the results with the minimum square of residual error, as stated by Markovsky [29]. The method used is by least squaring matrix $[A]$ by multiplying the transpose matrix itself $[A]^T$ so that matrix $[A]^T[A]$ has the same number of rows and columns. Matrix $[A]^T[B]$ will change the rows of matrix $[B]$ so that matrix $[B]$ has the same number of rows as $[A]^T$, as shown in Eq. (11). The variable values in matrix $[X]$ can be searched by multiplying the inverse matrix $[A^T A]^{-1}$ on both sides of the equation, as described in Eq. (10), which can be solved using mathematical software.

$$[A]^T[A] \times [X] = [A]^T[B] \quad (11)$$

$$[A^T A]^{-1} [A^T A] \times [X] = [A^T A]^{-1}[A]^T[B] \quad (12)$$

From Eq. (10), the values of $X \cong X_{LS}$ complying with the least squares method, called the unique least squares approximate solution, are defined as follows:

$$X_{LS} = [A^T A]^{-1} [A^T B] \quad (13)$$

Knowing the approximate values of X , acceptable approximation values of the separation efficiency of cyclones 2A, 3A, 4A, 2B, 3B and 4B can be calculated using the following equations:

$$\eta_{A2} = \frac{m_{sep-kf-2A}}{m_{sep-kf-1A} + m_{unsep_kf_2A}} \times 100\% \quad (14)$$

$$\eta_{A3} = \frac{m_{sep-kf-3A}}{m_{sep-kf-2A} + m_{unsep-kf-3A} - (\%Calc_{3A} * m_{gas-kf-A})} \times 100\% \quad (15)$$

$$\eta_{A4} = \frac{m_{sep-kf-4A}}{m_{kf-1L} - (\%Calc_{4A} * m_{gas-kf-A})} \times 100\% \quad (16)$$

$$\eta_{B2} = \frac{m_{sep-kf-2B}}{m_{sep-kf-1B} + m_{unsep_kf_2B}} \times 100\% \quad (17)$$

$$\eta_{B3} = \frac{m_{sep-kf-3B}}{m_{sep-kf-2B} + m_{unsep-kf-3B} - (\%Calc_{3B} * m_{gas-kf-B})} \times 100\% \quad (18)$$

$$\eta_{B4} = \frac{m_{sep-kf-4B}}{m_{kf-SL} - (\%Calc_{4B} * m_{gas-kf-B})} \times 100\% \quad (19)$$

The values of cyclone separation efficiency can be substituted into the mass conservation equation of each cyclone to recalculate the value of X that meets the mass conservation law. The final results of X can be used to evaluate the heat flow in each cyclone with minimum heat balance error (<1%) while tuning the values of gas and/or kiln feed temperatures if required. All the above-mentioned equations and calculation methods were adopted as the basis for developing a dedicated engineering equation solver (EES) software application and were used to calculate the detailed plant mass and heat flows.

2.4 Materials

The fuel used is fine coal, which is introduced into the plant through the ILC, the SLC, and the kiln burners. The average chemical compositions of the used fine coal and raw materials are presented in Table 1, while the other data required for the study, such as the geometry of the main equipment and the operation parameters, are presented in Tables 2, 3 and 4 respectively of Part 1 of this study [30].

3 Results and Discussion

3.1 Operation Data Parameters

The results of calculating the mass and heat balance in the SP and the calciners are given in Table 1. From the results, we can conclude that the difference between the outgoing and incoming heat rates is insignificant (0.64%). The percentage of calcined kiln feed in this SP is around 25% with around 8% in the cyclone 3 and the remaining 17% in the lowest cyclone (4).

Table 1 SP and calciner materials (kg) and heat (kcal) flows per kg of clinker.

Parameter	Inlet		Outlet	
	mass	heat	mass	heat
Kiln feed supplied to A and B strings	1.6659	22.780	-	-
Recirculating dust from kiln and cooler	0.2329	54.026	-	-
Fine coal supplied and combustion heat	0.1000	506.020	-	-
Total combustion air supplied	1.0926	218.219	-	-
Flue gas from kiln	0.635	174.496	-	-
Kiln feed gas from kiln	0.0810	21.873	-	-
Kiln feed to kiln	-	-	1.3110	299.324
Combustion gas including excess air	-	-	1.8400	181.365
Kiln feed gas out	-	-	0.5492	50.094
Return dust out of top cyclones	-	-	0.1072	9.950
Heat of calcination process	-	-	-	421.515
Evaporating of kiln feed water content	-	-	-	12.647
Convection and radiation loss	-	-	-	16.149
Total of materials and heat flows	3.8074	997.414	3.8074	991.044

The calculated results of mass and heat balances for strings A and B are presented in Tables 2 and 3 respectively. The results of calculating the separation efficiency of these cyclones depend on the measured temperature. For example, in cyclone 3, the temperature variation of material coming out of cyclone 2 as well as the gas entering cyclone 3 by $\pm 2^\circ\text{C}$ practically does not affect the value of its separation efficiency.

It should be noted that only the top cyclone is designed with high efficiency since its separation function is more dominant compared to its heat transfer function. Figure 2 shows the calculated results of cyclone separation efficiency for strings A and B that are impossible to measure directly in an operating plant. From this figure it can be seen that the separation efficiency is lower, the lower the position of the cyclone. This is in accordance with the previous statement that the separation function becomes less important and the heat transfer function between the gas and kiln feed particles becomes more dominant. This results also agrees with the design rule of thumb mentioned by FL Smidth [31] and Duda

SLCI Type Cement Plant (Part 2: Suspension Preheater & Calciners)

[32], who state that the material separation efficiency for the two lowest cyclones is around 80%.

Table 2 String A cyclone materials (kg) and heat (kcal) flows per kg of clinker.

Parameters	Cyclone 1A		Cyclone 2A		Cyclone 3A		Cyclone 4A	
	mass	heat	mass	heat	mass	heat	mass	heat
<i>Entering flow:</i>								
Kiln feed from upper cyclone	0.8584	11.738	0.9030	81.306	0.9890	148.281	-	-
Kiln feed dust from lower cyclone/ILC	0.1120	17.134	0.1980	38.297	0.2881	65.890	1.6010	366.44
Flue gas from lower cyclone	0.9824	147.77	0.9824	185.23	0.9824	217.97	-	-
Kiln feed gas from lower cyclone	0.2466	37.327	0.2466	47.550	0.2405	55.021	-	-
Flue gas from kiln	-	-	-	-	-	-	0.9824	218.25
Kiln feed gas from kiln	-	-	-	-	-	-	0.2386	54.730
Total of entering materials and heat flows	2.1994	213.97	2.3300	352.39	2.5000	487.16	2.8220	639.42
<i>Exiting flow:</i>								
Separated kiln feed	0.9030	81.306	0.9890	148.281	1.0730	206.158	1.3110	299.324
Unseparated dust flow to upper cyclone/duct	0.0550	5.091	0.1120	17.134	0.1980	38.297	0.2881	65.890
Kiln feed gas	0.2466	22.135	0.2466	37.327	0.2466	47.550	0.2405	55.021
Flue gas including excess air	0.9948	94.780	0.9824	147.769	0.9824	185.635	0.9824	217.971
Kiln feed vapor	-	7.341	-	-	-	-	-	-
Calcination heat	-	-	-	-	-	5.489	-	1.428
Heat loss	-	1.533	-	1.501	-	1.690	-	0.899
Total of exiting materials and heat flows	2.1994	212.19	2.3300	352.01	2.5000	484.82	2.8220	639.63

In addition to controlling the process, high efficiency in the top cyclone is meant to reduce pollutant emissions into the environment. However, for the 3 lower cyclones, the heat transfer function is more important. It can also be seen that the amount of heat carried by the exhaust gas from the top cyclones is significant (>200 kcal/kg of produced clinker). This heat can be recovered for drying lime stone and clay, as reported by Amalia, *et al.* [33,34]. The separation efficiency of the top cyclone is re-evaluated by Eqs. (5c) and (5d) in Part 1. The results of the cyclone mass and heat balance calculations are highly useful for designing new equipment, controlling the process, and modifying equipment. Some studies that

simulated the process in a calciner (Mikulčić, *et al.* [20,26] and Fidaros, *et al.* [35]) required data on the entering kiln feed flow that generally comes out of cyclone 3. Unfortunately, the origin of this data was not clearly explained and of course it cannot be measured directly in the plant. Using the simulation result presented in Tables 2 and 3, the process that occurs within the calciner is expected to be closer to real conditions.

Table 3 B-string cyclone materials (kg) and heat (kcal) flows per kg of clinker.

Parameters	Cyclone 1B		Cyclone 2B		Cyclone 3B		Cyclone 4B	
	mass	heat	mass	heat	mass	heat	mass	heat
<i>Entering flow:</i>								
Kiln feed from upper cyclone	0.8075	11.042	0.8570	79.258	0.8880	132.99	-	-
Kiln feed dust from SLC lower cyclone	0.1129	16.999	0.1440	27.631	0.3696	81.424	1.9240	427.94
Flue gas from lower cyclone	0.8409	129.98	0.8409	163.94	0.8409	187.62	-	-
Kiln feed gas from lower cyclone	0.3025	45.083	0.3025	57.782	0.3019	66.510	-	-
Flue gas from kiln	-	-	-	-	-	-	0.8410	189.35
Kiln feed gas from kiln	-	-	-	-	-	-	0.2951	65.624
Total of entering materials and heat flows	2.0638	203.10	2.1444	328.61	2.4004	468.54	3.0601	682.91
<i>Exiting flow:</i>								
Separated kiln feed	0.8570	79.258	0.8890	132.987	1.1130	212.963	1.5480	339.619
Unseparated dust flows to upper cyclone/duct	0.0520	4.859	0.1120	16.999	0.1440	27.631	0.3693	81.424
Kiln feed gas	0.3025	27.778	0.3025	45.083	0.3025	47.550	0.3019	66.510
Flue gas including excess air	0.8523	84.375	0.8409	129.979	0.8409	163.940	0.8409	187.623
Kiln feed vapor	-	4.827	-	-	-	-	-	-
Calcination heat	-	-	-	-	-	0.501	-	6.178
Heat loss	-	1.363	-	1.642	-	1.576	-	1.761
Total of exiting materials and heat flows	2.0638	202.46	2.1444	326.69	2.4004	463.89	3.0601	683.12

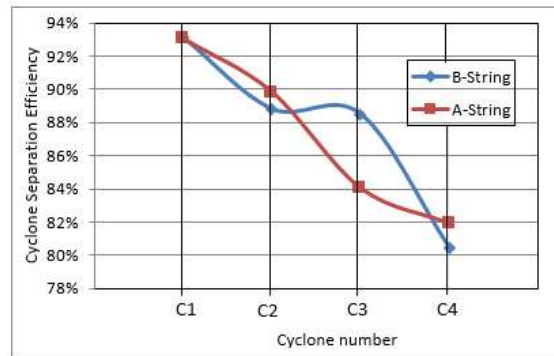


Figure 2 Calculated results of cyclone separation efficiency for strings A and B.

3.2 ILC and SLC Mass and Heat Flows

With the results of the calculation of the mass and heat balances in the SP's cyclones, especially C3 and C4, the calculation of the mass and heat balances in the calciners approaching real operating conditions were carried out. The results are shown in Table 4. These results are quite precise, with the difference between the heat in and out being less than 1%. The results of the mass and heat balances in the calciner are very useful for design, process simulation, equipment modification, calciner operational monitoring, and equipment maintenance. In addition, operation optimization by varying the fuel mass rate fed to the calciners that is associated with the degree of calcination of the kiln feed can be conducted.

Table 4 Materials (kg) and heat (kcal) flow per kg of clinker of ILC and SLC.

Parameters	ILC		SLC	
	mass	heat	mass	heat
<i>Entering mass and heat flows</i>				
Kiln feed from cyclone 3A	-	-	1.0730	206.158
Kiln feed from cyclone 3B	-	-	1.1130	212.963
Kiln feed from cyclone 4B	1.5480	339.619	-	-
Supplied fine coal and combustion heat	0.0290	146.852	0.0710	359.168
Combustion gas	0.3198	47.969	0.7800	170.249
Flue and kiln feed gas from kiln	0.7160	196.369	-	-
Dust from kiln and/or cooler	0.2097	49.284	0.0231	4.742
Total of mass and heat flow in	2.8225	780.093	3.0601	953.280
<i>Exiting mass and heat flows</i>				
Kiln feed to the cyclone 4A or 4B	1.6010	366.439	1.9240	427.940
Kiln feed gas	0.2389	54.730	0.2951	65.624
Flue gas including excess air	0.9826	218.247	0.8410	189.346
Heat of calcination process		142.371		265.548
Convection & radiation heat loss		1.671		2.513
Total of mass & heat flow out	2.8225	783.458	3.0601	950.971

For the example from Table 4, with fuel feeding rates of 9.13 TPH and 22.33 TPH in the ILC and the SLC respectively, the calculation result of the percentage of calcined kiln feed coming out of the ILC and the SLC was 85.3% and 56.3%, respectively, which is very difficult to obtain from direct measurement in the field because the calcination process cannot be stopped abruptly, even when quenching the kiln feed, because the process will still continue when the sample is taken until it is examined in the laboratory.

The estimated percentage and uniformity of the calcined kiln feed, especially when entering the kiln, greatly determines the quality of the clinker and closely influences the clinker microscopy. The clinker quality, which is normally determined by microscopic observation, significantly influences the quantity of a third material required when making Portland composite cement (PCC) so that the cement production process becomes more competitive, as reported by Darmanto and Amalia [36].

4 Conclusions

The advantage of the method proposed in this study is that it can estimate the materials flow and separation efficiency in each cyclone without measuring the flow rate, which is impossible in the field when the plant is operating. From this second part of the study, as presented in the paper, some conclusions that can be drawn are:

1. The estimated separation efficiency of each cyclone can be obtained with less than 0.9% error in the heat balance.
2. The proposed method can also be used to estimate the values of parameters that cannot be obtained by direct measurement in a running plant (e.g. cyclone efficiency, combustion air temperature exiting from the cooler, heat used for calcination in the calciners, and clinkerization heat).
3. The results obtained can be used as additional data in controlling operations, designing new equipment, as well as modifying the processes and dimensions of existing equipment.
4. The proposed method can also be applied to modern cement plants, which generally have calciners. Further analysis is required for different configurations of modern cement plants. However, the result reported in this work shows a good agreement between the calculation result and plant operation data.
5. The results of this study can contribute not only to controlling plant operation, but also for new equipment design, process improvement, and simulation of processes in the calciners.

Acknowledgment

The authors would like to express their gratitude and highest appreciation for the collaboration between PT Semen Padang and the Indonesian Cement and Concrete Institute for providing data from field observations for the case study in this paper.

References

- [1] Rivendra, R., Sudheer, B., Kumar, P., Suresh, J., Babu & Rajani Kant, D., *Detailed Energy Audit and Conservation in a Cement Plant*, International Research Journal of Engineering and Technology (IRJET), **2**(01), pp 248-256, 2015.
- [2] Anantharaman, N., *Heat Audit in Cement Industry (1500 tpd)*, International Journal of Science Technology & Engineering, **3**(10), pp. 12-18, 2017.
- [3] Avami, A. & Sattari, S., *Assessment of Heat Saving Opportunities of Cement Industries of Iran*, Proceedings of the 3rd IASME WISEAS International Conference on Heat, Environment, Ecosystem and Sustainable Development, Agios Nikoaios, Greece, pp. 585-593, 2007.
- [4] Khongprom, P. & Suwanmanee, U., *Environmental Benefits of the Integrated Alternative Technologies of the Portland Cement Production: A Case Study in Thailand*, Engineering Journal, **21**(7), pp. 15-27, 2017. DOI: 10.4186/ej.2017.21.7.15.
- [5] Nørskov, L.K., Dam-Johansen, K., Glarborg, P., Jensen, P.A. & Larsen, M.B., *Combustion of Solid Alternative Fuels in the Cement Kiln Burner*, Kgs. Lyngby: Technical University of Denmark (DTU), 2012.
- [6] Mikulčić, H., von Berg, E., Vujanović, M. & Duić, N., *Numerical Study of Co-firing Pulverized Coal and Biomass inside a Cement Calciner*, Waste Management & Research, **32**, pp. 661-669, 2014. DOI: 10.1177/0734242X14538309.
- [7] Chao C.Y., Kwong, P.C., Wang, J.H., Cheung, C.W., Kendall, G., *Co-firing Coal with Rice Husk and Bamboo and the Impact on Particulate Matters and Associated Polycyclic Aromatic Hydrocarbon Emissions*, Bioresour Technology, **99**(1), pp 83-93, 2008. DOI: 10.1016/j.biortech.2006.11.051
- [8] Kourounis, S. Tsivilis, S., Tsakiridis, P.E., Papadimitriou, G.D. & Tsibouki, Z., *Properties and Hydration of Blended Cements with Steelmaking Slag*, Cement and Concrete Research, **37**, pp. 815-822, 2007. DOI: 10.1016/j.cemconres.2007.03.008.
- [9] Varma A.B. & Gadling P.P., *Additive to Cement, A Pozzolanic Material-Fly Ash*, International Journal of Engineering Research, **5**(3), pp. 558-564, 2016.

- [10] Al-Chaar G.K, Alkadi M., Yaksic, D.A. & Kallemeyn, L.A., *The Use of Natural Pozzolan in Concrete as an Additive or Substitute for Cement*, ERDC/CERL TR-11-46, 2011. DOI:10.2174/1874836801307010033.
- [11] Allahverdi, A. & Salem, S.H., *Studies on Main Properties of Ternary Blended Cement with Limestone Powder and Microsilica*. Iranian Journal of Chemical Engineering, **4**(1), pp. 3-13, 2007.
- [12] Ayu, T.T., Hailu, M.H., Hagos, F.Y. & At Naw, S.M., 2015, *Heat Audit and Waste Heat Recovery System Design for a Cement Rotary Kiln in Ethiopia: A Case Study*, International Journal of Automotive and Mechanical Engineering (IJAME), **12**, pp. 2983-3002, 2015. DOI: 10.15282/ijame.12.2015.14.0249.
- [13] Riyanto, H. & Martowibowo, S.Y., *Optimization of Organic Rankine Cycle Waste Heat Recovery for Power Generation in a Cement Plant via Response Surface Methodology*, International Journal of Technology, **6**(6), pp. 938-945, 2015. DOI: 10.14716/ijtech.v6i6. 1695.
- [14] Kawasaki Plant System, Ltd., *Waste Heat Recovery Power Generation (WHRPG) for Cement Plant*, Heat Saving Seminar, Mexico, 2007.
- [15] Ali, A. & Mohammad, R.V., *Waste Heat Recovery Power Generation System for Cement Production Process*, IEEE Transaction on Industry Application, **51**(1), pp. 13-19, 2015.
- [16] Firman, B.J. & Muhammad, A., *Integrated System of Thermochemical Cycle of Ammonia, Nitrogen Production, and Power Generation*, International Journal of Hydrogen Energy, **44**(33), pp. 17525-17534, 2019. DOI: 10.1016/j.ijhydene.2019.05.110.
- [17] Firman, B.J., Darmanto, P.S. & Muhammad, A., *CO₂-free Power Generation Employing Integrated Ammonia Decomposition and Hydrogen Combustion-based Combined Cycle*, Thermal Science and Engineering Progress, **19**, 100672, 2020.
- [18] Paa, D.I. & Darmanto, P.S., *Numerical Study on the Influence of Rate of Kiln Feed On The Pressure Drop and Separated Efficiency of the Top Cyclone in Cement Plant*, Proceedings Seminar Nasional Tahunan Teknik Mesin XIII (SNTTM XIII), 2014. DOI: 10.1016/j.biortech.2006.11.051. (Text in Indonesian)
- [19] Darmanto, P.S., Astina, I.M. & Syahlan, A., *Design and Implementation of De-Duster for Improving Fine Coal Quality in a Cement Plant*. International Conference on Fluid and Thermal Heat Conversion (FTEC), Tongyeong, South Korea, 2009.
- [20] Mikulčić, H., Von Berg, E., Vujanović, M. & Duić, N., *Numerical Study of Co-Firing Pulverized Coal and Biomass Inside a Cement Calciner*, Waste Management & Research, **32**, pp. 661-669, 2014. DOI: 10.1177/0734242X14538309.
- [21] Amila, C.K., Morten, C.M. & Lars-André, T., *Numerical Modeling of the Calcination Process in a Cement Kiln System*, Proceedings of the 58th

SLCI Type Cement Plant (Part 2: Suspension Preheater & Calciners)

- SIMS, September 25th-27th, Reykjavik, Iceland, 2017. DOI: 10.3384/ecp1713883.
- [22] Grzegorz, B., Jacek, W. & Bolesław, D., *Modification of the Inlet to the Tertiary Duct in the Cement Kiln Installation*, Chemical and Process Engineering, **37**(4), pp. 517-527, 2016. DOI: 10.1515/cpe-2016-0042.
- [23] Claus B., *Modernization and Production Increase with Cement Kilns*, Humbolt Report, 2000.
- [24] Xavier D'Hubert, *Latest Burner Profiles*, Global Cement Magazine, **03**, 2017.
- [25] Niki G. & Akshey B., *Design of High Efficiency Cyclone for Tiny Cement Industry*, International Journal of Environmental Science and Development, **2**(5), pp. 350-354, 2011. DOI: 10.7763/IJESD.2011.V2.150.
- [26] Hrvoje, M., Von Berg, E., Milan, V., Peter, P., Reinhard, T. & Neven, D., *Numerical Analysis of Cement Calciner Fuel Efficiency and Pollutant Emissions*, Clean Tech Environ Policy, **15**, pp. 489-499, 2013. DOI: 10.1007/s10098-013-0607-5.
- [27] Copertaro, E., Chiariotti, P., Donoso, A.A.E., Paone, N., Peters, B. & Ravel, G.M., *A Discrete-Continuous Method for Predicting Thermochemical Phenomena in a Cement Kiln and Supporting Indirect Monitoring*, Engineering Journal, **22**(6), pp. 165-183, 2018. DOI: 10.4186/ej.2018.22.6.165.
- [28] Anton, H. & Rorres, C., *Elementary Linear Algebra*, 9th Edition, John Wiley and Sons Inc., United States, 2005.
- [29] Markovsky, I and Usevich, K., *Low Rank Approximation*, Communications and Control Engineering, , © Springer-Verlag London Limited , 2012. DOI 10.1007/978-1-4471-2227-2.
- [30] Darmanto, P.S., Muzakki, I.H., Astina, I.M, Juangsa, F.B., Amalia, A. & Syahlan, A., *New Method on the Materials Flow Calculation for Double Strings SLCI Type Cement Plant (Part 1: The Whole Clinker Plant)*, Journal of Engineering and Technological Sciences, **53**(5), 210506, 2021. DOI: 10.5614/j.eng.technol.sci.2021.53.5.6.
- [31] Smidth F.L, Plant Services Devison, *Heat Balances*, International Cement Production Seminar, Lecture 5.13A, FL Smidth Inc, 1990.
- [32] Duda, W.H., *Cement Data Book I*, 3rd edition, International Process in the Cement Industry, Bouverlag GmbH Weisbaden Und Berlin, 2000.
- [33] Amalia, A., Syahlan, A. & Darmanto, P.S., *Heat Auditing of Gresik and Tonasa Plants*, Internal Project Report of Indonesian Cement and Concrete Institute, 2017. (unpublished)
- [34] Amalia, A., Syahlan, A., and Darmanto, P.S., *Design and Implementation of Hot Gas System for Raw Coal Drying Process in Tonasa Plant*, Internal Project Report of Indonesian Cement and Concrete Institute, 2006. (unpublished)

- [35] Fidaros, D.K., Baxevanou, C.A., Dritselis, C.D. & Vlachos, N.S., *Numerical Modelling of Flow and Transport Processes in a Calciner For Cement Production*, Powder Technology, **171**, pp. 81-95, 2007. DOI: 10.1016/j.powtec.2006.09.011.
- [36] Darmanto P.S. & Amalia, A., *Analysis of High Clinker Ratio of Portland Composite Cement (PCC)*, South African Journal of Chemical Engineering, **34**, pp. 116-126, 2020. DOI: 10.1016/j.sajce.2020.07.010.

Appendix 1

Materials Flow Conservation Equations of Each Cyclone and Calcliner

A schematic diagram of the materials flow in the top cyclone for two strings is shown in Figure A1.

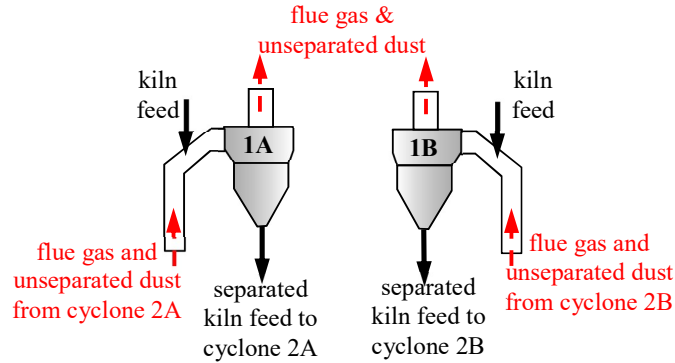


Figure A1 Flow diagram of materials flow in the top cyclones of strings A and B.

For the top cyclones, assuming zero flow leakage, the incoming mass flow consists of:

1. kiln feed at each string A and B, m_{kf-A} and m_{kf-B} at temperature T_{kf} .
2. flow of unseparated kiln feed from cyclones 2A and 2B, $m_{unsep-kf-2A}$ and $m_{unsep-kf-2B}$, where its temperature is T_{hg-2A} and T_{hg-2B} .
3. gas flow from the cyclone below temperature T_{hg-2A} and T_{hg-2B} , which consists of flue gas ($m_{hg-A}in$ & $m_{hg-B}in$) and kiln feed gas (CO_2 and others), ($m_{gas-kf-A}in$ and $m_{gas-kf-B}in$).

The outflow of mass from the top cyclones consist of:

1. separated kiln feed towards cyclones 2A and 2B, $m_{sep-kf-1A}$ and $m_{sep-kf-1B}$.
2. unseparated kiln feed at temperature T_{kf-1A} and T_{kf-1B} , ($m_{unsep-kf-1A}$ and $m_{unsep-kf-1B}$).
3. mass flow rate of evaporated water content in the kiln feed flowing through strings A and B, $m_{H2O-kf-1A}$ and $m_{H2O-kf-1B}$.
4. mass of flue gas through top cyclone of strings A and B, ($m_{hg-A}out$ and $m_{hg-B}out$).
5. mass of kiln feed gas of the calcination process through strings A and B, ($m_{gas-kf-A}out$ and $m_{gas-kf-B}out$).

The mass balance equation for the top cyclones of each string can be written as follows:

$$m_{kf-A} + m_{unsep-kf-2A} + (m_{hg-A}in) + (m_{gas-kf-A}in) = m_{sep-kf-1A} + m_{H2O-kf-1A} + m_{unsep-kf-1A} + (m_{hg-A}out) + (m_{gas-kf-A}out) \quad (A1)$$

$$m_{kf-B} + m_{unsep-kf-2B} + (m_{hg-B}in) + (m_{gas-kf-B}in) = m_{sep-kf-1B} + m_{H2O-kf-1B} + m_{unsep-kf-1B} + (m_{hg-B}out) + (m_{gas-kf-B}out) \quad (A2)$$

For general SP operation, the temperature of the gas that heats the kiln feed is slightly higher than the kiln feed temperature when exiting the cyclone (T_{kf-1A} and T_{kf-1B}). During operation of the plant, these temperatures are measured and can be read from the measurement mimic in the control room. The rate of the kiln feed and unseparated dust filtered by the baghouse can also be measured, assuming that the dust from cyclone 2 will

be filtered back by the top cyclone. Furthermore, the ratio of $(m_{kf-A} - m_{unsep-kf-1A})$ and m_{kf-A} can be used as an approach of the value of cyclone 1A separation efficiency, $\eta_{1.A}$. The same goes for cyclone 1B, $\eta_{1.B}$. In this case $(m_{gas-kf-A})_{in} = (m_{gas-kf-A})_{out}$ and $(m_{gas-kf-B})_{in} = (m_{gas-kf-B})_{out}$, while $(m_{hg-A})_{in} = (m_{hg-A})_{out}$ and $(m_{hg-B})_{in} = (m_{hg-B})_{out}$. Based on these operating conditions, the top cyclone separation efficiency can be approached with Eqs. (8a) and (8b). The heat balance of top cyclones 1A and 1B can be written as follows:

$$En_{kf-A} + m_{unsep-kf-2A} * h_{kf}(T_{hg-2A}) + m_{hg-A} * h_{hg}(T_{hg-2A}) + m_{gas-kf-A} * h_{CO_2}(T_{hg-2A}) = En_{hg-A} + En_{gas-kf-A} + En_{vapor-kf-A} + En_{unsep-kf-1A} + m_{sep-kf-1A} * h_{kf}(T_{kf-1}) + Q_{loss-1A} \quad (A3)$$

$$En_{kf-B} + m_{unsep-kf-2} * h_{kf}(T_{hg-2B}) + m_{hg-B} * h_{hg}(T_{hg-2B}) + m_{gas-kf-B} * h_{CO_2}(T_{hg-2B}) = En_{hg-B} + En_{gas-kf-B} + En_{vapor-kf-B} + En_{unsep-kf-1B} + m_{sep-kf-1B} * h_{kf}(T_{kf-1B}) + Q_{loss-} \quad (A4)$$

where $Q_{loss-1A}$ and $Q_{loss-1B}$ are heat loss by radiation and convection through the surface area of top cyclones 1A and 1B (A_{1A} and A_{1B}), which can be approached by Eq. (24) in Part 1 by substituting A_{tot} with A_{1A} and A_{1B} .

The flow of material in cyclones 2A and 2B is presented schematically in Figure A2. Using the same notation of materials and gas flow as denoted in Figure A2, the mass conservation equation of cyclones 2A and 2B can be written as follows:

$$m_{sep-kf-1A} + m_{unsep-kf-3} + (m_{hg-A})_{in} + (m_{gas-kf-A})_{in} = m_{sep-kf-2A} + m_{unsep-kf-2A} + (m_{hg-A})_{out} + (m_{gas-kf-A})_{out} \quad (A5)$$

$$m_{sep-kf-1} + m_{unsep-kf-3B} + (m_{hg-B})_{in} + (m_{gas-kf-B})_{in} = m_{sep-kf-2B} + m_{unsep-kf-2B} + (m_{hg-B})_{out} + (m_{gas-kf-B})_{out} \quad (A6)$$

while their heat conservation is represented by Eqs. (A7) and (A8).

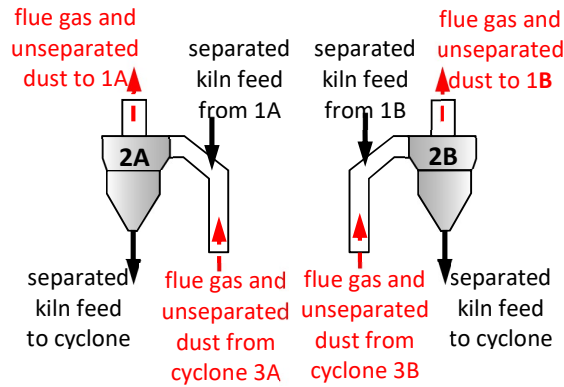


Figure A2 Flow of materials in the cyclones 2A and 2B.

$$m_{sep-kf-1A} * h_{kf}(T_{kf-1A}) + m_{unsep-kf-3} * h_{kf}(T_{hg-3A}) + m_{hg-A} * h_{hg}(T_{hg-3A}) + m_{gas-kf-A} * h_{CO}(T_{hg-3A}) =$$

SLCI Type Cement Plant (Part 2: Suspension Preheater & Calciners)

$$m_{hg-A} * h_{hg}(T_{hg-2A}) + m_{gas-kf-A} * h_{CO2}(T_{hg-2A}) + m_{unsep-kf-2} * h_{kf}(T_{hg-2A}) + m_{sep-kf-2A} * h_{kf}(T_{kf-2A}) + Q_{loss-2A} \quad (A7)$$

$$m_{sep-kf-1B} * h_{kf}(T_{kf-1B}) + m_{unsep-kf-3B} * h_{kf}(T_{hg-3B}) + m_{hg-B} * h_{hg}(T_{hg-3B}) + m_{gas-kf-B} * h_{CO2}(T_{hg-3B}) = m_{hg-B} * h_{hg}(T_{hg-2B}) + m_{gas-kf-B} * h_{CO2}(T_{hg-2B}) + m_{unsep-kf-2} * h_{kf}(T_{hg-2B}) + m_{sep-kf-2B} * h_{kf}(T_{kf-2B}) + Q_{loss-2B} \quad (A8)$$

A schematic flow diagram of materials in the third cyclones 3A and 3B is shown in Fig. A3 while their mass and heat balance are represented by Eqs. (A9)-(A12).

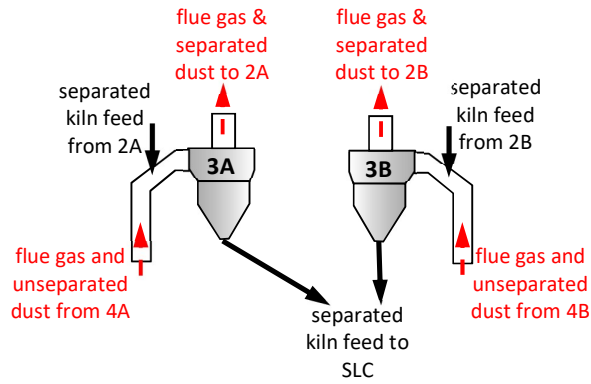


Figure A3 Flow of materials in the cyclones 3A and 3B.

$$m_{sep-kf-2A} + m_{unsep-kf-4} + (m_{hg-A})in + (m_{gas-kf-A})in = m_{sep-kf-3A} + m_{unsep-kf-3A} + (m_{hg-A})out + (m_{gas-kf-A})out \quad (A9)$$

$$m_{sep-kf-2B} + m_{unsep-kf-4} + (m_{hg-B})in + (m_{gas-kf-B})in = m_{sep-kf-3} + m_{unsep-kf-3} + (m_{hg-B})out + (m_{gas-kf-B})out \quad (A10)$$

In cyclones 3A and 3B, the calcination reaction of the kiln feed is started due to its temperature higher than 600 °C [31,32]. Part of the kiln feed forms CaO and CO₂. The formed CO₂ is equal to %Calc_{3A}*m_{gas-kf-A} in cyclone 3A and %Calc_{3B}*m_{gas-kf-B} in cyclone 3B. So the value of (m_{gas-kf-A})out = (m_{gas-kf-A})in + %Calc_{3A}*m_{gas-kf-A} and (m_{gas-kf-B})out = (m_{gas-kf-B})in + %Calc_{3B}*m_{gas-kf-B}.

$$m_{sep-kf-2A} * h_{kf}(T_{kf-2A}) + m_{unsep-kf-4} * h_{kf}(T_{hg-4A}) + m_{hg-A} * h_{hg}(T_{hg-4A}) + m_{gas-kf-A} * h_{CO2}(T_{hg-4A}) = m_{hg-A} * h_{hg}(T_{hg-3A}) + m_{gas-kf-A} * h_{CO}(T_{hg-3A}) + m_{unsep-kf-3} * h_{kf}(T_{hg-3A}) + m_{sep-kf-3A} * h_{kf}(T_{kf-3A}) + Q_{loss-3A} \quad (A11)$$

$$m_{sep-kf-2B} * h_{kf}(T_{kf-2B}) + m_{unsep-kf-4B} * h_{kf}(T_{hg-4B}) + m_{hg-B} * h_{hg}(T_{hg-4B}) + m_{gas-kf-B} * h_{CO2}(T_{hg-4B}) = m_{hg-B} * h_{hg}(T_{hg-3B}) + m_{gas-kf-B} * h_{CO}(T_{hg-3B}) + m_{unsep-kf-3B} *$$

$$h_{kf}(T_{hg-3B}) + m_{sep-kf-3} * h_{kf}(T_{kf-3B}) + Q_{loss-3B} \quad (A12)$$

In Eqs. (A11) and (A12) $En_{calc-3A} = \%Calc_{3A} * En_{calc}$ and $En_{calc-3B} = \%Calc_{3B} * En_{calc}$ are the heat of the calcination process in cyclones 3A and 3B.

Figure A4 shows a schematic diagram of the materials flow in cyclones 4A and 4B. The mass and heat balance of these cyclones are represented by Eqs. (A13)-(A16).

$$m_{kf-ILC} + (m_{hg-A})in + (m_{gas-kf-A})in = m_{sep-kf-k} + m_{unsep-kf-4} + (m_{hg-A})out + (m_{gas-kf-A})out \quad (A13)$$

$$m_{kf-S} + (m_{hg-B})in + (m_{gas-kf-B})in = m_{sep-kf-ILC} + m_{unsep-kf-4} + (m_{hg-B})out + (m_{gas-kf-B})out \quad (A14)$$

Similar to cyclones 3A and 3B, the calcination reaction of the kiln feed continues in cyclones 4A and 4B. The formed CO₂ is equal to $\%Calc_{4A} * m_{gas-kf-A}$ and $\%Calc_{4B} * m_{gas-kf-B}$ in these cyclones. So the value of $(m_{gas-kf-A})out - (m_{gas-kf-A})in = \%Calc_{4A} * m_{gas-kf-A}$ and $(m_{gas-kf-B})out - (m_{gas-kf-B})in = \%Calc_{4B} * m_{gas-kf-B}$.

$$\begin{aligned} m_{kf-I} * h_{kf}(T_{kf-ILC}) + m_{hg-A} * h_{hg}(T_{hg-IL}) + m_{gas-kf-A} * h_{CO2}(T_{hg-IL}) \\ = m_{hg-A} * h_{hg}(T_{hg-4A}) + m_{gas-kf-A} * h_{CO2}(T_{hg-4A}) \\ + m_{unsep-kf-4} * h_{kf}(T_{hg-4A}) + m_{sep-kf-k} * h_{kf}(T_{kf-4A}) + \\ En_{calc-} + Q_{loss-} \end{aligned} \quad (A15)$$

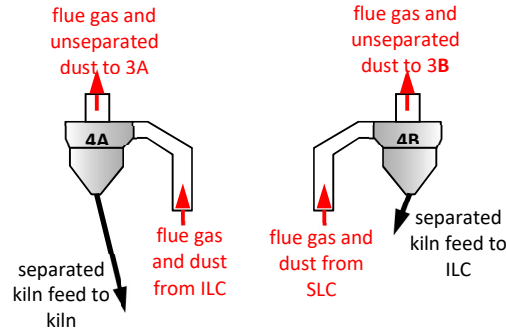


Figure A4 Flow of materials in the cyclones 4A and 4B.

In the Eqs.(A15) and (A16) $En_{calc-4A} = \%Calc_{4A} * En_{calc}$ and $En_{calc-4B} = \%Calc_{4B} * En_{calc}$ are the heat of the calcination process in the cyclones 4A and 4B previously mentioned in Eq. (9).

$$\begin{aligned} m_{kf-SLC} * h_{kf}(T_{kf-SLC}) + m_{hg-B} * h_{hg}(T_{hg-SL}) + m_{gas-kf-B} * h_{CO2}(T_{hg-SL}) \\ = m_{hg-B} * h_{hg}(T_{hg-4B}) + m_{gas-kf-B} * h_{CO}(T_{hg-4B}) \\ + m_{unsep-kf-4} * h_{kf}(T_{hg-4B}) + m_{sep-kf-ILC} * h_{kf}(T_{kf-4B}) \\ + En_{calc-} + Q_{loss-4B} \end{aligned} \quad (A16)$$

For the ILC and the SLC, the schematic diagram of material flows is presented in Fig. A5. Based on this figure, the equation of mass balance of the ILC and the SLC are given

SLCI Type Cement Plant (Part 2: Suspension Preheater & Calciners)

by Eqs. (A17) and (A18) respectively, while Eqs.(A19) and (A20) are their related heat balance equations.

$$m_{sep-kf-4B} + m_{hg-k-ILC} + m_{clid-k-IL} + m_{comb-air-IL} + m_{clid-c-IL} + m_{coal-ILC} + m_{tr-air-ILC} = m_{kf-I} + m_{hg-IL} + m_{gas-kf-ILC} \quad (A17)$$

$$m_{sep-kf-3B} + m_{sep-kf-3B} + m_{comb-air-SL} + m_{clid-c-SLC} + m_{coal-SLC} + m_{tr-air-SL} = m_{kf-SLC} + m_{hg-SLC} + m_{gas-kf-SLC} \quad (A18)$$

$$\begin{aligned} & m_{sep-kf-4B} * h_{kf}(T_{kf-4B}) + En_{hg-k-ILC} + En_{clid-k-ILC} + En_{comb-air-ILC} \\ & + En_{clid-c-ILC} + En_{tr-air-ILC} + En_{coal-comb-IL} + En_{coal-ILC} \\ & = m_{kf-I} * h_{kf}(T_{hg-IL}) + En_{evap-H2O-coal-A} + \\ & m_{hg-IL} * h_{hg}(T_{hg-ILC}) + m_{gas-kf-ILC} * h_{CO2}(T_{hg-ILC}) + Q_{loss-ILC} \end{aligned} \quad (A19)$$

$$\begin{aligned} & m_{sep-kf-3A} * h_{kf}(T_{kf-3A}) + m_{sep-kf-3B} * h_{kf}(T_{kf-3}) + En_{comb-air-SLC} \\ & + En_{clid-c-SLC} + En_{tr-air-SL} + En_{coal-comb-SLC} + En_{coal-SLC} \\ & = m_{kf-SLC} * h_{kf}(T_{hg-SLC}) + En_{evap-H2O-coal-B} + \\ & m_{hg-SL} * h_{hg}(T_{hg-SL}) + m_{gas-kf-SLC} * h_{CO} (T_{hg-SLC}) + Q_{loss-SLC} \end{aligned} \quad (A20)$$

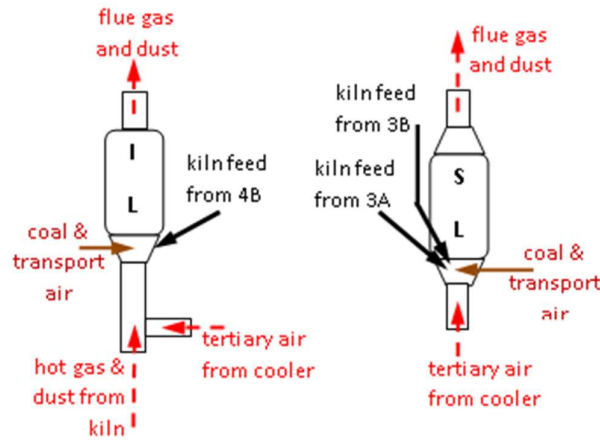


Figure A5 Flow of materials in the ILC and the SLC.

It should be noted that in Eq. (A17) mass flow rate of flue gas from the ILC (m_{hg-ilc}) is equal to the mass flow rate of flue gas entering to string A of SP (m_{hg-A}) in mentioned in Eq. (A13), while the flow rate of kiln feed gas resulted by calcination in the ILC ($m_{gas-kf-ILC}$) is equal to $\{(m_{hg-A})_{in} - m_{hg-k-ILC}\}$. From the mass balance of the SLC (Eq. A18), it can be deduced that the flow rate of the kiln feed gas resulted by calcination $m_{gas-kf-SLC} = \%Calc_{SLC} * m_{gas-kf} = \{(m_{hg-B})_{in} - m_{hg-SLC}\} = \{(m_{hg-B})_{in} - ((1-ash_{coal}) * m_{coal-SLC} + m_{comb-air-SLC} + m_{tr-air-SLC})\}$. In Eqs. (A19) and (A20), T_{kf-ILC} , T_{hg-ILC} , T_{kf-SLC} and T_{hg-SLC} are respectively temperature of kiln feed and gas exiting the ILC and the SLC.

Appendix 2

Element of Matrices [A], [B], and [X]

$$[A] = \begin{bmatrix} 1 & 0 & -1 & 0 & 0 & 0 & 0 & 0 & 0 & 0 & 0 & 0 & 0 \\ h_{kf}(T_{kf-2A}) & 0 & -h_{kf}(T_{hg-3A}) & 0 & 0 & 0 & 0 & 0 & 0 & 0 & 0 & 0 & 0 \\ -1 & 1 & 1 & -1 & 0 & 0 & 0 & 0 & 0 & 0 & 0 & 0 & 0 \\ -h_{kf}(T_{kf-2A}) & h_{kf}(T_{kf-3A}) & h_{kf}(T_{hg-3A}) & -h_{kf}(T_{hg-4A}) & 0 & 0 & 0 & 0 & 0 & 0 & 0 & 0 & 0 \\ 0 & 0 & 0 & 1 & -1 & 0 & 0 & 0 & 0 & 0 & 0 & 0 & 0 \\ 0 & 0 & 0 & h_{kf}(T_{hg-4A}) & -h_{kf}(T_{hg-ILC}) & 0 & 0 & 0 & 0 & 0 & 0 & 0 & 0 \\ 0 & 0 & 0 & 0 & 1 & 0 & 0 & 0 & 0 & -1 & 0 & 0 & 0 \\ 0 & 0 & 0 & 0 & h_{kf}(T_{hg-ILC}) & 0 & 0 & 0 & 0 & -h_{kf}(T_{kf-4B}) & 0 & 0 & 0 \\ 0 & 0 & 0 & 0 & 0 & 1 & 0 & 0 & -1 & 0 & 0 & 0 & 0 \\ 0 & 0 & 0 & 0 & 0 & h_{kf}(T_{kf-2B}) & 0 & -h_{kf}(T_{hg-3B}) & 0 & 0 & 0 & 0 & 0 \\ 0 & 0 & 0 & 0 & 0 & -1 & 1 & 1 & 0 & 0 & -1 & 0 & 0 \\ 0 & 0 & 0 & 0 & 0 & -h_{kf}(T_{kf-2B}) & h_{kf}(T_{kf-3B}) & h_{kf}(T_{hg-3B}) & 0 & -h_{kf}(T_{hg-4B}) & 0 & 0 & 0 \\ 0 & 0 & 0 & 0 & 0 & 0 & 0 & 0 & 0 & 1 & 1 & -1 & 0 \\ 0 & 0 & 0 & 0 & 0 & 0 & 0 & 0 & 0 & h_{kf}(T_{kf-4B}) & h_{kf}(T_{hg-4B}) & -h_{kf}(T_{hg-5LC}) & 0 \\ 0 & -1 & 0 & 0 & 0 & 0 & -1 & 0 & 0 & 0 & 0 & 1 & 0 \\ 0 & -h_{kf}(T_{kf-3A}) & 0 & 0 & 0 & 0 & -h_{kf}(T_{kf-3B}) & 0 & 0 & 0 & 0 & h_{kf}(T_{hg-5LC}) & 0 \end{bmatrix}$$

$$[B] = \begin{bmatrix} m_{sep-kf-1A} - m_{unsep-kf-2A} \\ m_{sep-kf-1A} * h_{kf}(T_{hg-1A}) + m_{hg-A} * \{h_{hg}(T_{hg-3A}) - h_{hg}(T_{hg-2A})\} + \\ m_{gas-kf-A} * \{h_{CO2}(T_{hg-3A}) - h_{CO2}(T_{hg-2A})\} - m_{unsep-kf-2A} * h_{kf}(T_{hg-2A}) - Q_{loss-2A} \\ - \%Calc_{3A} * m_{gas-kf-A} \\ m_{hg-A} * \{h_{hg}(T_{hg-4A}) - h_{hg}(T_{hg-3A})\} + m_{gas-kf-A} * \{h_{CO2}(T_{hg-4A}) - h_{CO2}(T_{hg-3A})\} - \\ En_{calc-3A} - Q_{loss-3A} \\ m_{sep-kf-k} - \%Calc_{4A} * m_{gas-kf-A} \\ m_{hg-A} * \{h_{hg}(T_{hg-4A}) - h_{hg}(T_{hg-ILC})\} + m_{gas-kf-A} * \{h_{CO2}(T_{hg-4A}) - h_{CO2}(T_{hg-ILC})\} + \\ m_{sep-kf-k} * h_{kf}(T_{hg-4A}) - En_{calc-4A} - Q_{loss-4A} \\ - m_{clid-k-ILC} - m_{clid-c-ILC} - \%Calc_{ILC} * m_{gas-kf-A} + \%ash_{coal} * m_{coal-ILC} \\ En_{clid-k-ILC} + En_{clid-c-ILC} + En_{hg-k-ILC} + En_{com-air-ILC} - m_{hg-ILC} * h_{hg}(T_{hg-ILC}) - \\ m_{gas-kf-ILC} * h_{CO2}(T_{hg-ILC}) + En_{evap-H2O-coal-ILC} - En_{coal-ILC} - \\ En_{calc-ILC} + En_{coal-comb-ILC} - Q_{loss-ILC} \\ m_{sep-kf-1B} - m_{unsep-kf-3B} \\ m_{sep-kf-1B} * h_{kf}(T_{hg-1B}) + m_{hg-B} * \{h_{hg}(T_{hg-3B}) - h_{hg}(T_{hg-2B})\} + \\ m_{gas-kf-B} * \{h_{CO2}(T_{hg-3B}) - h_{CO2}(T_{hg-2B})\} - m_{unsep-kf-2B} * h_{kf}(T_{hg-2B}) - Q_{loss-2B} \\ - \%Calc_{3B} * m_{gas-kf-B} \\ m_{hg-B} * \{h_{hg}(T_{hg-4B}) - h_{hg}(T_{hg-3B})\} + m_{gas-kf-B} * \{h_{CO2}(T_{hg-4B}) - h_{CO2}(T_{hg-3B})\} - \\ En_{calc-3B} - Q_{loss-3B} \\ - \%Calc_{4B} * m_{gas-kf-B} \\ m_{hg-B} * \{h_{hg}(T_{hg-4B}) - h_{hg}(T_{hg-5LC})\} + m_{gas-kf-B} * \{h_{CO2}(T_{hg-4B}) - h_{CO2}(T_{hg-5LC})\} + \\ m_{sep-kf-ILC} * h_{kf}(T_{hg-4B}) - En_{calc-4B} - Q_{loss-4B} \end{bmatrix}$$

$$[X] = \begin{bmatrix} m_{sep-kf-2A} \\ m_{sep-kf-3A} \\ m_{unsep-kf-3A} \\ m_{unsep-kf-4A} \\ m_{kf-ILC} \\ m_{sep-kf-2B} \\ m_{sep-kf-3B} \\ m_{unsep-kf-3B} \\ m_{sep-kf-4B} \\ m_{unsep-kf-4B} \\ m_{kf-5LC} \end{bmatrix}$$